ISBN: 978-3-95450-238-7 ISSN: 2226-0358 doi:10.18429/JACoW-ICALEPCS2023-TUPDP005

IMPROVEMENTS ON KINEMATICS AND CONTROL OF GRANITE BENCHES AT LNLS-SIRIUS*

J. V. E. Matoso†, J. P. S. Furtado, J. P. B. Ishida, T. R. S. Soares
Brazilian Synchrotron Light Laboratory, Campinas, Brazil

Abstract

At the Brazilian Synchrotron Light Laboratory, the radiation beam is conditioned by optical elements that must be positioned with high stability and precision. Many of the optical elements are positioned using granite benches that provide high coupling stiffness to the ground and position control in up to six degrees of freedom, using a set of stepper motors. The solution of the inverse kinematics was done numerically by the Newton Raphson method. By employing the property that these systems have small rotation angles, the Jacobian matrix used in this numerical method can be simplified to reduce computational execution time and allow high processing rates. This paper also shows the results of adding a notch filter to the position servo control loop of the granite benches to increase stability due to their mass-spring-damper characteristics. The kinematics and control of the granite benches are implemented in an Omron Power Brick LV controller, with the kinematics developed in MATLAB and the C-code generated by MATLAB C-Coder. Reducing the execution time of the kinematics improves the efficient use of the computational resources and allows the real-time clock rate to be increased.

INTRODUCTION

Granite benches have many applications in the Sirius beamlines, such as positioning mirrors, monochromators, and experimental stations, providing high mechanical and thermal stability [1, 2].

The latest granite bench design has seven motors and six degrees of freedom (Fig. 1). The system consists of a stack of three granite pieces. The first layer is supported by three levelers that provide translation in Y and rotations along the X and Z axes. The next two layers of granite together provide rotation along the Y axis and translations in the X, Y and Z axes. These layers are positioned using a system of belts and pulleys driven by stepper motors. To reduce friction, the granites have air bearings to guide and lift the granite layers.

This article presents the latest advances in the calculation of the inverse kinematics of this mechanism since the last article [3] and introduces a new discussion on the position control of air-bearing granites using belt and pulley systems. All kinematic calculations and motor control are performed on an Omron Delta Tau Power Brick LV controller.

Figure 1: Mirror granite bench design used as a reference.

KINEMATICS

Model Overview

The kinematic calculations of this system are divided into two parts: the closed-chain tripod formed by the three levelers; and the remaining open-chain robot with 7 axes formed by the resulting effect of the levelers plus the movement of the granites (Fig. 2). The tripod kinematics for the levelers will not be covered in this article. For more information, see [3].

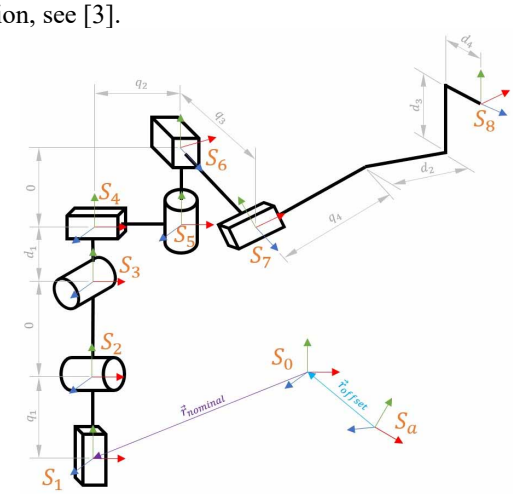

Figure 2: Mirror system kinematic scheme [3].

The control point is located at the S_8 coordinate system with coordinates $\vec{u}$ relative to the coordinate system S_0 fixed on the beam, where $\vec{f}$ is the forward kinematics and $\vec{e}$ the axes positions. The axes $R_{x_{lev}}, R_{z_{lev}}$ and $T_{y_{lev}}$ are

* Work supported by the Ministry of Science, Technology & Innovation.
† joao.matoso@lnls.br

ISBN: 978-3-95450-238-7 ISSN: 2226-0358 doi:10.18429/JACoW-ICALEPCS2023-TUPDP005

computed beforehand using the forward kinematics for the tripod levelers system.

$$\vec{u} = \vec{f}(\vec{e}) = (R_x, R_y, R_z, U_x, U_y, U_z)$$

where: $\vec{e} = (R_{x_{lev}}, R_{z_{lev}}, T_{y_{lev}}, R_{y_{bench}}, T_x, T_w, T_z)$

The solution to the inverse kinematics problem proposed by [3] is based on the Newton's method and consists of solving the following system of equations $\vec{G}(\vec{e}_k, \vec{u}_{des})$:

$$\vec{G}(\vec{e}, \vec{u}_{des}) = \vec{u}_{des} - \vec{f}(\vec{e}) = 0$$

Where $\vec{u}_{des}$ is the desired pose of the mirror bench and $\vec{e}$ is the vector of axes positions. By Newton's method, each iteration computes a new iteration of $\vec{e}_k$ until the norm of the error vector $\vec{G}$ is less than the encoder resolution.

$$\vec{e}_{k+1} = \vec{e}_k - \mathcal{J}_G^{-1}(\vec{e}_k) \cdot \vec{G}(\vec{e}_k, \vec{u}_{des})$$

Where $\mathcal{J}_G^{-1}(\vec{e}_k)$ is the inverse Jacobian matrix of $\vec{G}(\vec{e}_k, \vec{u}_{des})$. The forward kinematics equations are found by combining simple homogeneous transformations matrices, and then calculating the rotations using the Euler angle conventions. Until the last work presented, the Jacobian matrix was calculated symbolically, as well as its inverse, using the Sympy library in Python [4]. In this way, we obtained long equations that solved Newton's method in about 2,156 ms using an Omron Power Brick with a PowerPC CPU.

Simplified Numerical Solution

The mirror's granite benches have a very small angular range. For example, the first mirror (M1) of the SABIA beamline has only ±20 mrad for rotations along the X and Z axes, and ±60 mrad for rotations along the Y axis. As the inverse kinematics should only work correctly for these small angles, we can linearize the equations that compute the Jacobian matrix by applying the first-order Taylor polynomial at the point $(R_{x_{lev}}, R_{y_{bench}}, R_{z_{lev}}) = (0,0,0)$, and we obtain the linearized form $\mathcal{J}_G^*(\vec{e})$. Then, the new iterative equation is computed as below:

$$\vec{e}_{k+1} = \vec{e}_k - \mathcal{J}_G^{*-1}(\vec{e}_k) \cdot \vec{G}(\vec{e}_k, \vec{u}_{des})$$

Since the Jacobian matrix is now an approximation of the original matrix for small angles, the further away from zero the angles are, the more iterations are required for Newton's method to converge, and we can no longer guarantee that the method will converge for all angles.

Validation and Performance Tests

To verify the convergence of the method for the entire bench workspace and measure the performance, a benchmark test is developed to measure the number of iterations required to converge and the total time required to reach the solution of 78125 points equally spaced over the 7 input variables workspace, for both methods, using the Omron Power Brick LV with a PowerPC CPU.

The test results are shown in Table 1. The values are the average of the 78125 different calculations performed. As expected, the simplified method takes more iterations to converge. However, the simplified equations are simpler to calculate, and the total time taken to calculate the inverse kinematics is reduced by 95,6%.

Table 1: Inverse Kinematic Methods Comparison

Method	Iterations	Total Time [µs]
Original	2,34	2156,0
Simplified	3,13	95,5

CONTROL OF GRANITE BENCHES

Dynamic Model

To design a position controller for the granite bench system, a first approach consists of developing a dynamic model. The system can be modeled as a mass sliding over a surface with viscous friction, actuated by timing belts that are modeled as linear springs (Fig. 3) [5].

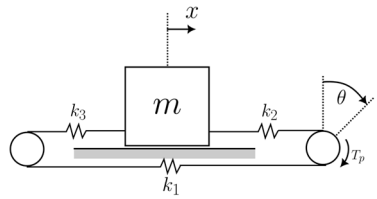

Figure 3: Dynamic model for the granite mechanism.

Considering m the total mass of granite and vacuum chamber, J the moment of inertia of the drive pulley, k_1, k_2, k_3 the stiffness constant equivalent to the timing belt, r the pulley radius, c_x the damping coefficient of the interface between the granite pieces, c_p the damping coefficient associated with the pulley system, T_p the torque input from the motor, x the granite position, θ the pulley position and k_t torque proportionality constant, the state space representation of the system $\dot{X} = AX + Bu$, $y = CX + Du$ is:

$$A = \begin{pmatrix} 0 & 0 & 1 & 0 \\ 0 & 0 & 0 & 1 \\ \frac{-8k_1}{3m} & \frac{8k_1 r}{3m} & \frac{-c_x}{m} & 0 \\ \frac{8k_1 r}{3J} & \frac{-8k_1 r^2}{3J} & 0 & \frac{-c_p}{J} \end{pmatrix}$$

$$B = \begin{pmatrix} 0 & 0 & 0 & \frac{k_t}{J} \end{pmatrix}^T$$

$$C = (1 \quad 0 \quad 0 \quad 0) \text{ and } D = (0)$$

with $X = (x \quad \theta \quad \dot{x} \quad \dot{\theta})^T$

This dynamic model is obtained using Lagrange's mechanical equations along with Rayleigh's dissipation function. It is assumed that the linear springs are made of the same material and have the same cross-sectional area and by Hooke's law: $k_2 = k_3 = 2 \cdot k_1$.

ISBN: 978-3-95450-238-7 ISSN: 2226-0358 doi:10.18429/JACoW-ICALEPCS2023-TUPDP005

From this model, it can be concluded that the main dynamics of this system can be expressed by a transfer function with four poles and no zeros.

System Identification

A system identification is carried out to identify a transfer function with four poles and no zeros, from the input $u(t)$, which is the open-loop speed command for the stepper motor, to the output $y(t)$, which is the position of the granite layer.

The excitation signal $u_e(t)$ is defined as a periodic square wave signal varying in amplitude, as shown in (Fig. 4). The amplitudes chosen are in the system's usual working region (up to 0.05 revolutions per second). The signals are written and acquired at a rate of 1 kHz.

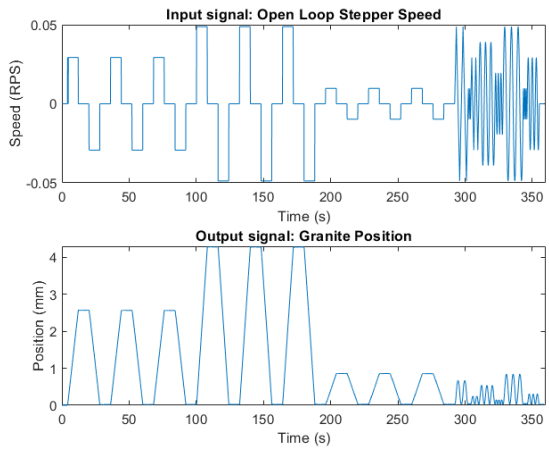

Figure 4: Excitation signal and response used to estimate transfer function.

From the system excitation signal and position data, the following transfer function is estimated, where $G(s) = Y(s)/U(s)$. The units of Y(s) are in encoder counts, where one count is equivalent to 500 nm, and the units of U(s) are in µsteps per servo cycle, where one servo cycle is 1 ms.

$$G(s) = \frac{5{,}133 \cdot 10^6}{s^4 + 41{,}72s^3 + 711{,}3s^2 + 24140}$$

Finally, the identified plant response can be compared with new data acquired from the plant, as shown in (Fig. 5). The total root mean square error (RMSE) between the model response and the plant response is 13 µm. As the highlight shows, the model can reproduce the oscillations that occur at around 3,8 Hz in the positioning of the granite.

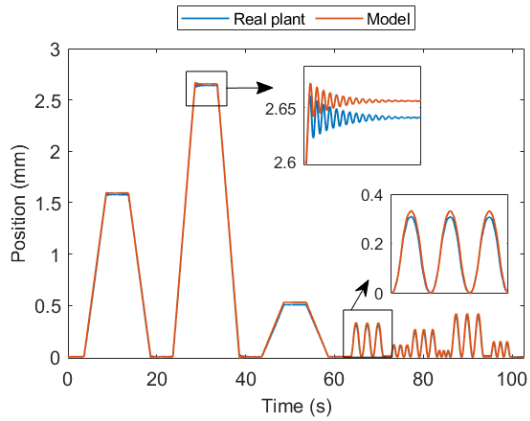

Figure 5: Comparison between model and plant responses.

Control Design

In this section, the main objective is to obtain some insight into how to choose a good filter and calculate the proportional gain of a position controller. The main requirements for this controller, in relation to a step response, are:

- Zero steady-state error.
- Stabilization time less than 5 seconds.
- No overshoot.

The transfer function identified has four poles at the following locations: $p = (0 \quad -39{,}26 \quad -1{,}23 \pm 24{,}77)$ rad/s, as seen in the root locus diagram (Fig. 6).

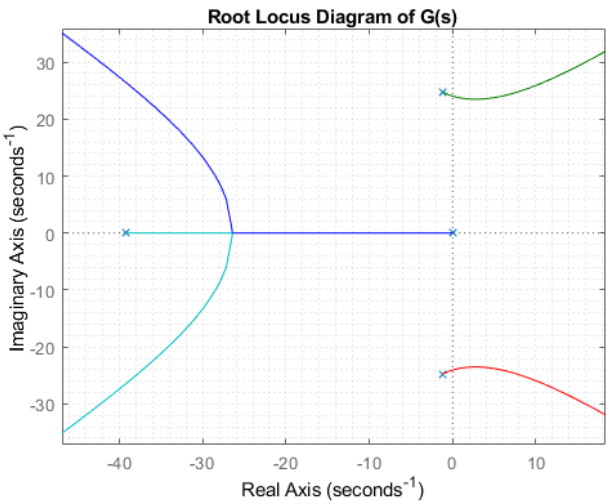

Figure 6: Root locus diagram of the identified transfer function.

ISBN: 978-3-95450-238-7 ISSN: 2226-0358 doi:10.18429/JACoW-ICALEPCS2023-TUPDP005

Assuming a simple proportional controller $C(s) = k_p$, the highest possible k_p value that still keeps the system stable, i.e. keeps the system poles in the negative real part, is 0,0149. In practice, this value cannot be used, as the system would never stabilize.

Analysis of the root locus diagram shows the negative influence of the pair of complex poles present in the $G(s)$. In order to counteract the effect of these poles on position control, a notch filter can be designed at their frequency.

By choosing the notch frequency ω_c at 24,7 rad/s, with a magnitude gain at $H_{notch}(j\omega_c) = -20$ dB, the transfer function for the notch is shown below:

$$H_{notch}(s) = \frac{s^2 + 4{,}96s + 615}{s^2 + 49{,}6s + 615}$$

The root locus diagram for $G(s) \cdot H_{notch}(s)$ is represented in the (Fig. 7). By applying the notch filter to the frequency of the complex poles, the controller reduces the effect of these poles, reducing the resonance at a frequency of 24,8 rad/s. Then, the controller $C(s)$ is chosen to be:

$$C(s) = k_p \frac{s^2 + 4{,}96s + 615}{s^2 + 49{,}6s + 615}$$

By choosing the proportional gain as $k_p = 0{,}014328$, the most significant poles of the system are positioned in a manner that gives the fastest response to the step, without overshooting.

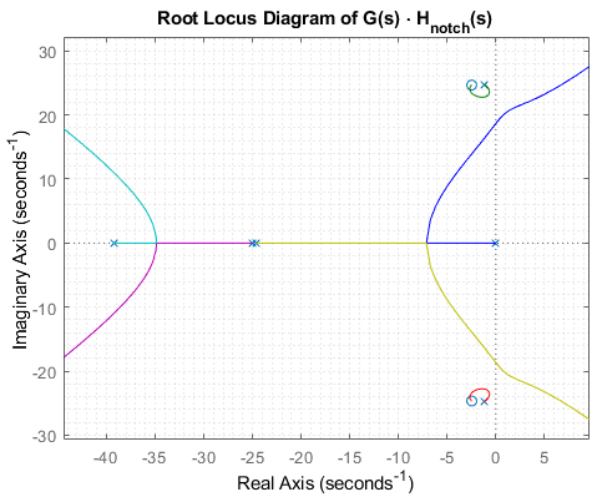

Figure 7: Root locus diagram for plant and notch filter

Control Validation

The $C(s)$ controller is discretized using the zero-pole matching equivalent, for a servo control loop rate of 1 kHz, which gives the following $C(z)$ transfer function:

$$C(z) = 14{,}01 \cdot 10^{-3} \cdot \frac{1 - 1{,}994 \cdot z^{-1} + 0{,}995 \cdot z^{-2}}{1 - 1{,}951 \cdot z^{-1} + 0{,}952 \cdot z^{-2}}$$

This controller is embedded into the Power Brick LV using the C code generated in Simulink. The (Fig. 8) shows the plant's step response to a 50 µm step. It can be concluded that the three design requirements are met by this controller: no overshoot, zero error in steady state and settling time less than 5 seconds.

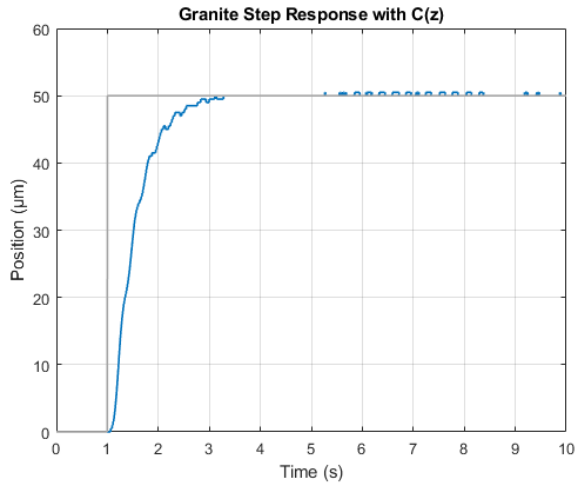

Figure 8: Granite step response with the notch filter.

CONCLUSION

Granite benches have a complex kinematic calculation due to the large number of axes (7 motors) and the combination of an open-chain robot with a closed-chain "tripod" kinematics. The simplification takes advantage of the small range of angles of these benches and reduces the total time needed to find a solution by 95,6%. With this reduction, these calculations consume less controller processing time and make it possible to increase the real time rate if necessary.

Along with the kinematic simplification, a new approach to controlling the position of the granite layers lifted by air-bearings is introduced by applying a Notch filter to the system's resonance frequency. This approach has proved effective in stabilizing the system and its resonance frequency can be easily identified in the field.

REFERENCES

[1] R. R. Geraldes *et al.*, "Granite Benches for Sirius X-ray Optical Systems", in *Proc. MEDSI'18*, Paris, France, Jun. 2018, pp. 361-364. doi:10.18429/JACoW-MEDSI2018-THPH12

[2] R. R. Geraldes *et al.*, "The Design of Exactly-Constrained X-Ray Mirror Systems for Sirius", in *Proc. MEDSI'18*, Paris, France, Jun. 2018, pp. 173-178. doi:10.18429/JACoW-MEDSI2018-WEOAMA04

[3] G. N. Kontogiorgos, A. Y. Horita, L. Martins dos Santos, M. A. L. Moraes, and L. F. Segalla, "The Mirror Systems Benches Kinematics Development for Sirius/LNLS", in *Proc. ICALEPCS'21*, Shanghai, China, Oct. 2021, pp. 358-361. doi:10.18429/JACoW-ICALEPCS2021-TUPV001

[4] SymPy, https://www.sympy.org/

[5] J. V. E. Matoso, "Desenvolvimento de sistema de controle para movimentação de bases de granito para o posicionamento de espelhos ópticos", final report for the Faculty of Mechanical Engineering, UNICAMP, Campinas, Brazil, 2022.